Third International Conference on CFD in the Minerals and Process Industries
CSIRO, Melbourne, Australia
10-12 December 2003

THE USE OF COUPLED SOLVERS FOR COMPLEX MULTI-PHASE AND REACTING FLOWS

I P JONES[1], P W GUILBERT[1], M P OWENS[1], I S HAMILL[1], C A MONTAVON[1], J M T PENROSE[1] and B PRAST[2]

[1] ANSYS CFX, Harwell Business Centre, Didcot, Oxon OX11 0QR, UK
[2] TWISTER BV, Einsteinlaan 10, 2289 CC Rijswijk, The Netherlands.

ABSTRACT

Many of the problems encountered in the minerals and process industries are very complex, with strong interactions between phases and components. This paper describes the extension of the coupled solvers used in the CFX-5 software to some flows of this type, including the use of Population Balance models to predict size distributions of a disperse phase, and illustrates the results on some practical industrial problems. Some verification and validation of the results is also described.

NOMENCLATURE

r_α : disperse phase volume fraction
N : number of groups
f_i : MUSIG volume fraction
n_i : number of bubbles of volume v_i per unit volume
B_C :birth by coalescence
D_C :death by coalescence
B_B : birth by break-up
D_B : death by coalescence
G_{ij} : Break-up rate from volume j to volume i
$G_i = \sum_{k=1}^{i} G_{ki}$: Break-up rate from volume i
Q_{ij} : coalescence rate for a pair with volume i and volume j

INTRODUCTION

The use of 'Implicit Coupled Solver' methods in the CFX-5 software has been a great success for single-phase flows, and they have enabled much more robust convergence to be obtained than when using segregated solvers. The original formulation, Raw [1], applied them to the mass conservation and momentum equations for single-phase flows. One important reason for their success is the use of a robust Algebraic Multi-Grid (AMG) method, which solves the equation system and is almost linear with the number of variables. This implies that the method is very scalable to large grid sizes. Because of its implicit nature, the method is also applicable to a wide range of flow speeds, from slow viscous flows to high Mach numbers.

This method has since been extended to Multi-Phase flows using the Eulerian Multi-Fluid approach [2], and similar convergence rates have been observed to those for single phase flows.

Many of the problems encountered in the minerals and process industries are very complex, with strong interactions between phases and components, for example mass transfer and chemical reactions. This paper describes the extension of the coupled solvers to some flows of this type, including Population Balance models to predict size distributions of a dispersed flow, and illustrates the results on some practical industrial problems:

- Bubble Columns
- The Twister™, a novel device for the separation of condensable components from a gas stream.

Some related validation and verification of these models is also described.

POPULATION BALANCE MODELS

Two-Fluid Models

The standard two-fluid model uses a single particle size to determine the inter-phase drag. It can be extended to a size distribution for a disperse phase, where the particle sizes are known, by adding additional 'fluids', each one representing a different particle size. This can be expensive for many fluids, as each fluid has its own velocity field. In many applications, for droplets and bubbles, the size distribution is not known a-priori, and it is necessary to predict the distribution in order to determine any heat and mass transfer, and subsequent chemical reactions.

The size distribution for the dispersed phase can be predicted using a population balance model, also known as the MUSIG (MUltiple SIze Group) model in CFX-4 [3]. A single disperse phase is characterized by various size groups, from which a local Sauter mean diameter is deduced. In the initial work, all the disperse-phase droplets were assumed to share the same velocity field, with the interphase drag determined from the Sauter mean diameter of the local size distributions. This is a reasonable assumption for bubbly flows, and liquid-liquid flows, where the disperse phase tends to have a 'swarm' velocity. This has since been extended to account for multiple velocity fields in the work described later in this paper on gas-droplet flows.

Basic Implementation

The 'droplets' in the disperse phase interact and change size due to the processes of break-up and coalescence. The disperse phase is discretised in N size groups with typically an equal mass or an equal diameter distribution. The method aims to solve for the volume fraction for each size group, f_i .

The equation representing the birth and death processes can be written as:

$$\frac{\partial}{\partial t}(r_\alpha \rho_\alpha f_i) + \nabla \cdot (r_\alpha \rho_\alpha \underline{U}_\alpha f)_i = S_i$$

with the source terms:

$$S_i = B_{i,B} - D_{i,B} + B_{i,C} - D_{i,C}$$

2.2.1 Break-up:

$$B_{i,B} = r_\alpha \rho_\alpha \sum_{j=i+1}^{N} G_{ij} f_j$$

$$D_{i,B} = r_\alpha \rho_\alpha G_i f_i \qquad \text{with} \qquad G_i = \sum_{k=1}^{i} G_{ki}$$

2.2.2 Coalescence:

$$B_{i,C} = r_\alpha^2 \rho_\alpha \cdot \frac{1}{2} \sum_{m=1}^{i} \sum_{k=1}^{i} Q_{mk} f_m f_k \frac{v_m + v_k}{v_m v_k} D_{mki}$$

$$D_{i,C} = r_\alpha^2 \rho_\alpha f_i \sum_{i+m<N} Q_{im} \frac{f_m}{v_m} = r_\alpha^2 \rho_\alpha f_i \sum_{m=1}^{N} Q_{im} \frac{f_m}{v_m} \sum_{k=1}^{N} D_{imk}$$

where the matrix D_{ijk} is defined by the discretisation such that:

$$D_{ijk} = \begin{cases} 1 \text{ if } m_i + m_j > m_k \\ 0 \text{ otherwise} \end{cases}$$

For the implementation of the coupled solution, we need in addition to the source term itself, the Jacobian of the source term, in order to perform a proper linearisation of the system.

The Jacobian of the source term S_i is defined as $\frac{\partial S_i}{\partial f_j}$

and will have contributions from the break-up and coalescence birth and death terms, such that:

$$\frac{\partial S_i}{\partial f_j} = \frac{\partial B_{i,B}}{\partial f_j} - \frac{\partial D_{i,B}}{\partial f_j} + \frac{\partial B_{i,C}}{\partial f_j} - \frac{\partial D_{i,C}}{\partial f_j}$$

These individual contributions will be:

$$\frac{\partial B_{i,B}}{\partial f_j} = \rho_\alpha r_\alpha G_{ij} \qquad \text{for j > i}$$

$$= 0 \qquad \text{otherwise}$$

$$\frac{\partial D_{i,B}}{\partial f_j} = \rho_\alpha r_\alpha \delta_{ij} \sum_{k=1}^{i} G_{ki}$$

$$\frac{\partial B_{i,C}}{\partial f_j} = \rho_\alpha r_\alpha^2 \sum_{k=1}^{i} f_k Q_{jk} \frac{v_j + v_k}{v_j v_k} D_{jki}$$

$$\frac{\partial D_{i,C}}{\partial f_j} = \rho_\alpha r_\alpha^2 \left\{ Q_{ij} \frac{f_i}{v_j} \sum_{k=1}^{N} D_{ijk} + \delta_{ij} \sum_{l=1}^{N} Q_{il} \frac{f_l}{v_l} \sum_{k=1}^{N} D_{ilk} \right\}$$

The implementation of the source terms in CFX-5 is such that, in every element, at every coefficient loop, the volume fraction changes associated with the death by break-up/coalescence compensate the volume fraction changes associated with the birth by break-up/coalescence.

Various models have been implemented for the calculation of the break-up and coalescence rates. The overall form of these models is similar, with different correlations used for coalescence and break-up depending on the nature of the flow. Models have been implemented for liquid-gas systems, and liquid-liquid systems, such as in suspension polymerisation. In the latter case, the rheology of the droplets is very important, and influences the break-up and coalescence. The specific models that have been implemented for the break-up rate are:

- Luo and Svendsen [4] for bubbly flows
- Droplets where the drop is a Power Law fluid (Vivaldo-Lima et al [5])
- Droplets where the drop is a Maxwell fluid (Maggioris et al [6], Alvarez et al [8])

For the coalescence, the following models are available:

- Prince and Blanch for bubbly flows[7]
- Power Law model (Vivaldo-Lima et al, [5])
- Maxwell model (Maggioris et al [6])

Break-Up Model

Luo and Svendsen developed a theoretical model for the break-up of drops and bubbles in turbulent dispersions. The model is based on the theories of isotropic turbulence, and significantly contains no unknown or adjustable parameters. The details of the model are also described in [3]. For the Maxwell and Power Law models, the birth and death terms due to break-up in the population balance are given by the following:

$$G_{ij} = \beta(v_j) n_d(v_j) \xi(v_j, v_i)$$

where $n_d(v_j)$ represents the number of daughter drops formed from the breakage of a mother drop with volume v_j. $\xi(v_j, v_i)$ represents the daughter drop distribution.

$\beta(v)$ corresponds to the breakage rate, which is usually modelled as follows:

$$\beta(v) = \omega_b(v) e^{-\lambda_b(v)}$$

where $\omega_b(v)$ is the breakage frequency of a droplet with volume v and $\lambda_b(v)$ denotes the efficiency of breakage.

Further information on the correlations implemented can be found in Montavon[9].

Coalescence Model

The coalescence of two bubbles is often assumed to occur in three steps. First the bubbles collide trapping a small amount of liquid between them. This liquid film then drains until the liquid film separating the bubbles reaches a critical thickness. The film ruptures and the bubbles join together. Prince and Blanch considered the collisions resulting from three different mechanisms: turbulence, buoyancy and laminar shear.

For the Maxwell and Power Law models, the coalescence rate distribution is modelled as:

$$Q_{ij} = \omega_c(v_i, v_j) e^{-\lambda_c(v_i, v_j)}$$

where $\omega_c(v_i,v_j)$ is the coalescence frequency of two droplets with volumes v_i and v_j , and $\lambda_c(v_i, v_j)$ denotes the efficiency of coalescence. This coalescence efficiency for droplets depends on the rheology of the droplets.

The detailed correlations implemented are beyond the scope of this paper, and will be described separately. They have been used extensively for prediction of reacting flows in mixing vessels, for example, suspension polymerisation processes,(see Montavon [9]).

Extension to Multi-Component Condensation

If condensation is taking place onto droplets in the disperse phase, then size change can also occur because of birth due to nucleation and size change due to condensation and evaporation. The modelling of these processes is outlined later in this paper.

A further extension carried out has been to implement the Population Balance Model for multi-component condensation, for the Twister™ work described later. This has required the implementation of non-equilibrium thermodynamics models for the multi-component gas, and a general framework for the inclusion of multiple species in the disperse phase into the Population Balance methodology. With this extension, each size band at a particular location is assumed to have the same average composition, and the mass of each component present in the liquid phase at this location is also computed. The overall approach can therefore lead to very large systems of equations, and therefore efficiency and robustness is very important.

NUMERICAL IMPLEMENTATION

In order to make these complex models tractable to use, great care has to be taken in the detailed numerical implementation, to give a robust and efficient implementation for both serial and parallel solution.

CFX-5 uses an implicit ‘coupled solver’ approach to solve the momentum and mass conservation equations simultaneously. The success of the method depends on a robust implementation of the Algebraic Multi Grid (AMG) method. For single-phase flows this has been very successful, and it has been extended to multi-phase flows using the multi-fluid model, for a single drop or bubble size (Yin et al [2]). This implementation shows similar convergence rates to the single-phase equations, unlike segregated methods.

Initially the population balance models were implemented in a ‘segregated’ manner, as in CFX-4, solving each equation sequentially, and iterating around to get convergence. The testing of the method indicated that:

- The equation systems can be very stiff, with a lot of cancellation between similar sized terms.
- There is no mechanism to prevent the individual MUSIG groups from overshooting or undershooting when the source terms are large, which typically occurs with large rates or large time steps.

In the work described here, the coupled solver method has been extended to the population balance models. The population balance equations presented above were linearised with respect to the solution variables as described earlier, to give a coupled set of convection-diffusion equations. This set of equations is then solved using the same coupled implicit Algebraic Multi Grid method used for the momentum equations.

Detailed testing of the method on a wide range of problems has shown:

- Solving the system in a fully coupled way helps significantly in reducing the overshoot and undershoot problems
- Larger time steps can be used, thereby speeding up convergence.

The example shown in Figure 1 compares the convergence results for the segregated and the coupled approach for an idealised example in a bubble column. This demonstrates the much more reliable convergence with fewer iterations and the non-oscillatory behaviour obtained through the coupled approach.

Because the AMG method also is efficient in parallel, the overall method parallelises well.

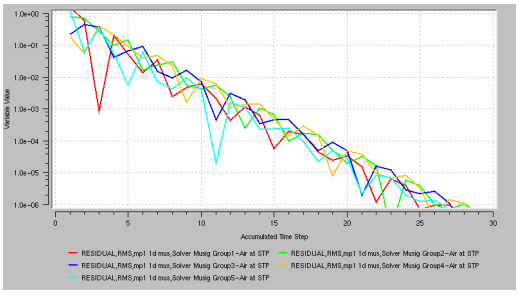

Figure 1a: Convergence History, Uncoupled solver

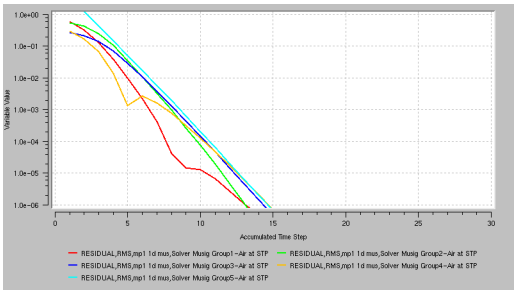

Figure1b: Convergence History, Coupled Solver

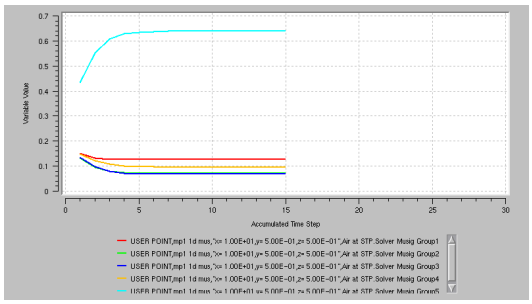

Figure1c: Monitor Values, Coupled Solver

APPLICATIONS

The population balance models have been implemented and tested on several different applications, including bubble columns, mixing vessels and Twister™. Validation of these complex multi-phase models can be very difficult, because of the lack of detailed experimental information on size distributions, and the need to calibrate the models.

Bubble Columns

Previously, the MUSIG model was implemented in CFX-4, and it has been extensively tested on a wide range of applications and test cases. The main testing reported in this paper for bubble columns therefore focuses on verification of the model implementation, with comparisons between CFX-4 and CFX-5. Figure 2 shows a comparison between CFX-4 and CFX-5 for the distribution of the Sauter Mean Diameter, with good agreement between the two implementations. Similar agreement has been found for other cases.

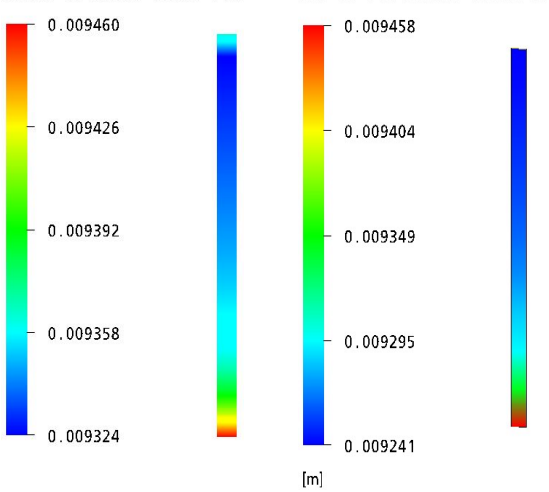

Figure 2: Bubble Column, Sauter Mean Diameter
a) CFX-4 b) CFX-5

Twister

Twister BV [10] develops and delivers compact gas processing units for dew pointing purposes and the recovery of natural gas liquids. Twister BV also provides consultancy services in hydrocarbon multiphase flow modelling. Twister technology is a combination of known physical processes, with characteristics similar to those of a Turbo-Expansion / Compression system.

Gas is expanded adiabatically in a Laval nozzle, creating supersonic velocities and low temperatures (for example a temperature at inlet of 20°C drops mid-Twister™ to -50°C). The low temperature creates a fog-like condensation, which is typically a mixture of water and heavier hydrocarbons. Still at supersonic velocities, the mixture of gas and liquid droplets enters a wing section, generating a high velocity swirl. The resulting swirl forces the condensate outward to form a liquid film on the inner wall of the tube. The liquid film is then removed using either a co-axial tube or slits in the wall of the separation tube. The dry gas core remains as the primary stream. After inducing a weak shock wave, 70 to 80 percent of the initial gas pressure is recovered using a diffuser. Figure 3 illustrates the Twister™ device, and the various flow regimes.

This is a very challenging application, involving high speed flows and strong swirl, as well as multi-component condensing flows. Further background information on Twister™ can be found in [11].

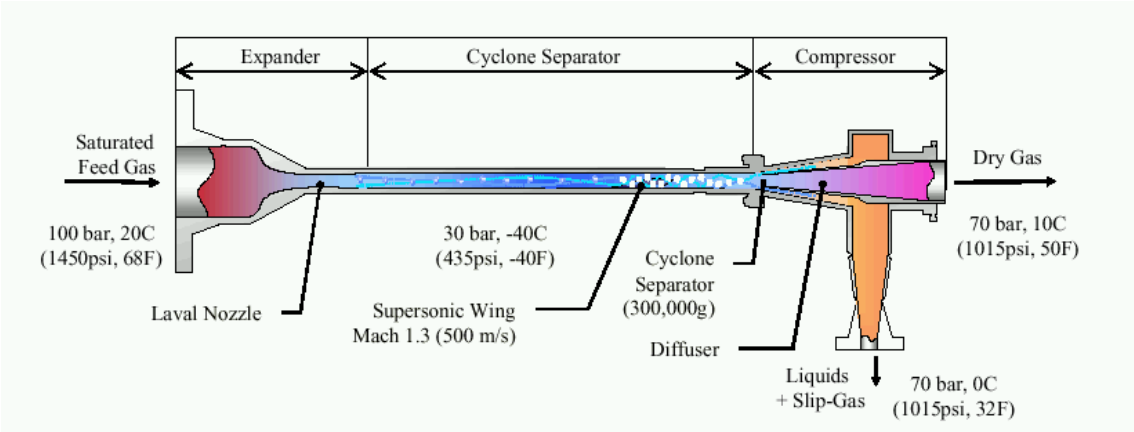

Figure 3: Schematic Representation of the Twister™

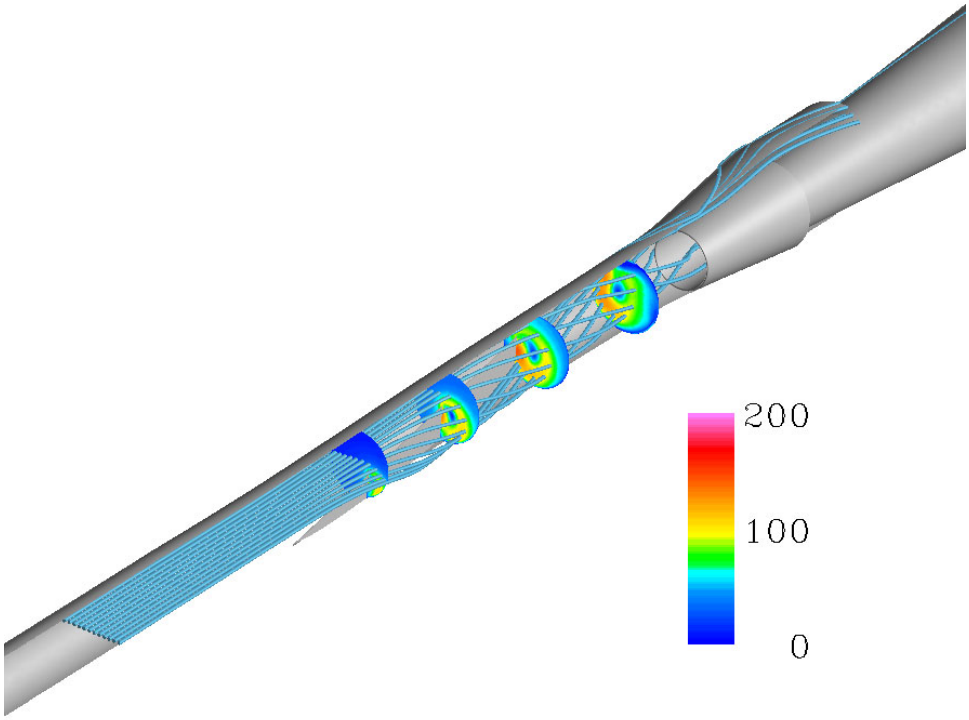

Figure 4: Streamlines and speed contours illustrating the highly swirling flow in Twister™.

Figure 4 shows the streamlines for the pure gas flow in Twister™, which illustrates the swirling and compressible flow nature in Twister™.

An enhanced model has been developed to model the Twister™. This consists of several basic steps:

- Multi-component non-ideal gas properties, using non-equilibrium thermodynamics, to give a correct representation of the flow properties under the large pressure and temperature variations.
- Nucleation model, to provide the seed for further growth.
- Growth modelling, to allow the liquid to condense onto the small drops.
- Multi-phase model, to allow differential motion between the gas, and the droplets.
- Droplet slip, break-up and coalescence.

Nucleation

The underlying physics is similar to that described in detail by Luitjen [12], Lamanna [13] and used in CFX-TASCflow, (Gerber [14]). This calculates an initial drop size, based on the Gibbs free energy required to overcome the barrier to forming small nucleated droplets and a number density for the nucleating particles. Any one of several species are allowed to nucleate in the implementation.

Growth

The growth rate is determined by the collisions between vapour molecules and liquid clusters. The probability no longer includes the nucleation energy barrier factor as there are stable clusters on which to condense.

Transport Modelling

Previous work in condensing gases has used the Lagrangian particle tracking approach to compute the trajectories of droplets, once they become large enough to slip relative to the gas. In the present work, the influence of swirl and turbulence can be important. In particular, the particles that are separated are very small, of the order of microns. In order to take turbulence into account, a large number of samples would be required to get converged statistics with a stochastic method such as the Eddy Lifetime approach. It was decided therefore to base the model upon an Eulerian Population Balance model, where the particle size distribution is discretised into a number of bands. As outlined above, this was extended to include the multi-component nature of the fluids, by including the condensable components. This greatly increases the number of variables that have to be solved, so again, efficiency is very important.

For this application, the droplets are very small, and the droplet relaxation time is very small. In this case, the Algebraic Slip Model (ASM) is appropriate, as an algebraic relationship can be used to calculate the slip velocity. This greatly simplifies the modelling and the subsequent computational resources. In the model, therefore, each size group has its own velocity field, so the separation of different drop sizes can be studied.

The main non-linearity in this case is in the nucleation and growth processes, as there can be very rapid changes in the condensation properties resulting in sharp condensation fronts. The coupled solver has therefore been applied to nucleation and growth into the lowest size band, as this is the most non-linear part of the process. Without this treatment, the convergence was found to be significantly harder to achieve.

Model Verification And Validation

Luijten [12] and Lamanna [13] have carried out extensive studies of the condensation processes in Laval nozzles. There is very little detailed experimental work available for detailed validation. Figures 5a and 5b show a comparison against experiment for two different configurations of the 'G1' Laval nozzle for the density along the axis. The experiment and predictions are in good agreement outside the condensation front. For the fronts themselves, the width of the condensation fronts are similar, with density changes of a similar magnitude.

Lamanna has carried out a detailed numerical study of the same nozzle, which indicate the results are very sensitive to the details of the nucleation and growth models. The current comparison with experiment are very similar to her findings. A detailed discussion is given by Lamanna of the sensitivity of the various models for this case

Further verification work has therefore focused on comparisons with the numerical results of Lamanna, for condensation of water vapour in a Laval Nozzle. Two different nozzles were tested, the G1 and the G2 nozzles. Figures 6 and 7 show a comparison between the work of Lamanna and the present work for the nucleation rate and the droplet radius, which shows that for the same models, the results are in good agreement. Similar agreement has been obtained for other detailed quantities, such as the rate of droplet growth. For this reason, they are not shown here. Lamanna did not consider the effects of droplet size and slip. To illustrate the effects of the slip and break-up modelling, two computations have been carried out for the G1 nozzle, with and without break-up. Figures 8a and b show the mass fraction in two size bands. These show the sharp condensation front, with larger droplets being created near this front, but disappearing downstream. This is due to the break-up caused by the shear between the droplets and the mean gas flow. In Figures 9a and 9b, the break-up model was turned off. In this case, the model shows that the larger droplets persist downstream, and they are not broken up.

CONCLUDING REMARKS

This paper has studied some complex multi-phase industrial flows, particularly for population balance modelling for the prediction of droplet and bubble size distributions, and has demonstrated the benefits that can accrue from judicious use of implicit coupled solvers. Only limited experimental information with the required level of detail is available, The results are consistent with the limited experimental work, and in good agreement with other available numerical work. These models are now being used to develop new and improved designs of the industrial applications studied.

ACKNOWLEDGEMENTS

This work was part-funded by the European Commission's Optimum project, contract number G1RD-CT-2000-00263, and by Twister BV.

REFERENCES

1. M J RAW, Robustness of Coupled Algebraic Multigrid for the Navier-Stokes Equations Presented at 34th Aerospace Sciences Meeting, Reno, Nevada, January 15-18, AIAA-Paper 96-0297, 1996.
2. D.L. YIN, A. BURNS, A. SPLAWSKI, C.GUETARI, (2001), Fourth International Conference on Multiphase Flow. New Orleans, Louisiana, U.S.A., May 27 – June 1, 2001, - paper number 1191
3. CFX-4.4 User Manual, AEA Technology, 2001.
4. H LUO and H SVENDSEN, (1996), AICHE J., Vol 42, No 5, pp 1225-1233.
5. E. VIVALDO-LIMA, P.E. WOOD, A.E. HAMIELEC, A. PENLIDIS, (1997), An updated review on suspension polymerization, Ind. Eng. Chem. Res. 36, pp 939-965.
6. D. MAGGIORIS, A. GOULAS, A.H. ALEXOPOULOS, E.G. CHATZI, C. KIPARISSIDES, (2000) Chem. Eng. Sci. 55, pp 4611-4627.
7. M J PRINCE and H W BLANCH, (1990) AICHE J., Vol 36, No 10, pp 1485-1499.
8. J. ALVAREZ, J. ALVAREZ, M. HERNANDEZ, (1994) Chem. Eng. Sci. . 49(1), pp 99-113.
9. C A MONTAVON, In preparation.
10. http://www.twisterbv.com

11. http://www.twisterbv.com/downloads/SPE_83977_Twister.pdf
12. C C M LUIJTEN, Nucleation and Droplet Growth at High Pressure, PhD thesis, University of Eindhoven,1998.
13. G LAMANNA, On Nucleation and Droplet Growth, PhD thesis, University of Eindhoven, 2000.
14. A GERBER, CFX TASCflow Prototype capability Condensing Steam Model, Version 2.7 Internal AEA Document, 1997.

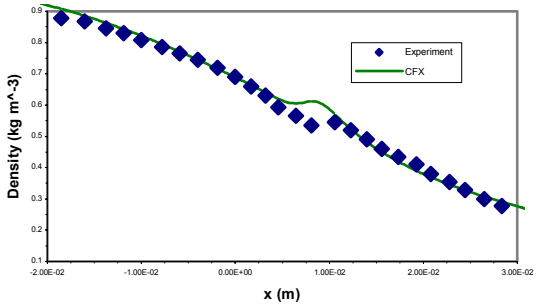

Figure 5a: Density along the axis of the G1 Laval Nozzle, Comparison with experimental results (S0=0.928)

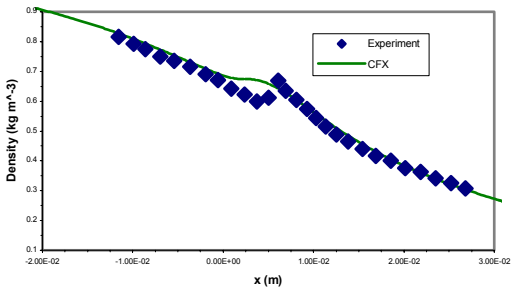

Figure 5b: Density along the axis of the G1 Laval Nozzle, Comparison with experimental results (S0=1.24)

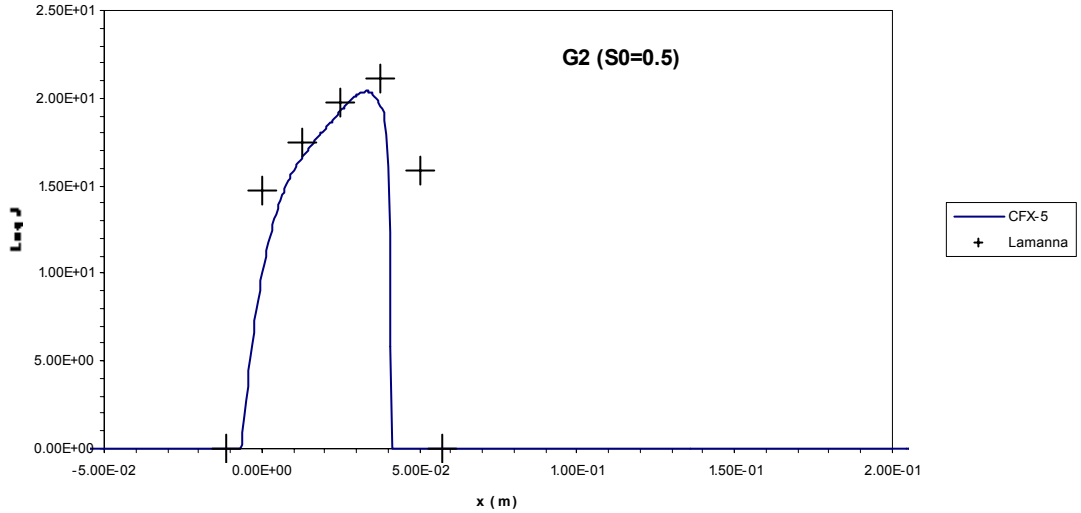

Figure 6: Comparisons between the Numerical Results of Lamanna, and the current work for log of the nucleation rate, G2 Nozzle.

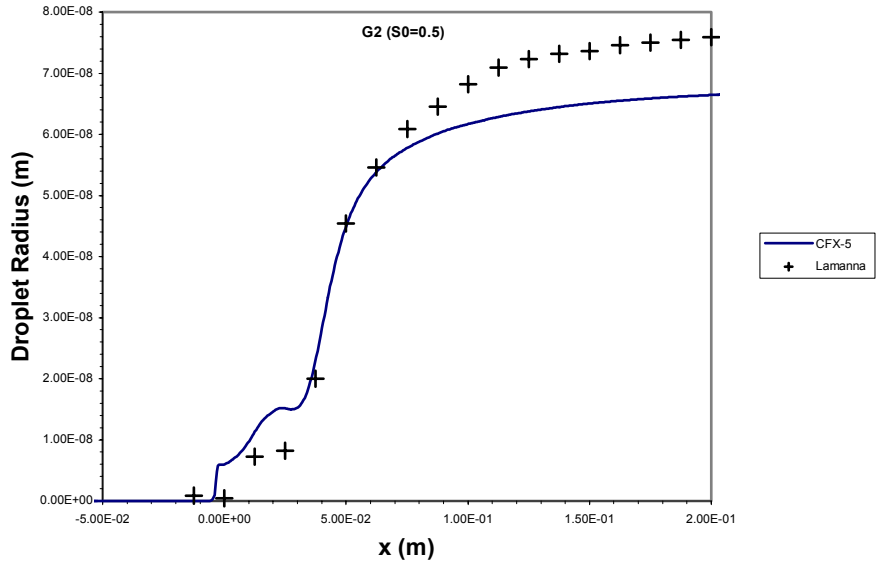

Figure 7: Comparisons between the Numerical Results of Lamanna, and the current work for droplet radius, G2 Nozzle.

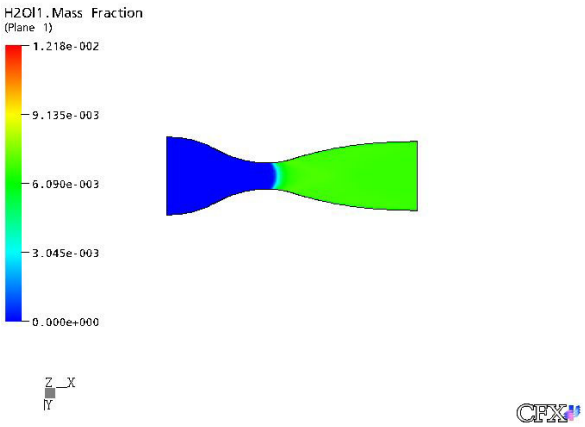

Figure 8: Liquid Mass Fraction, Band 1, G1 Nozzle

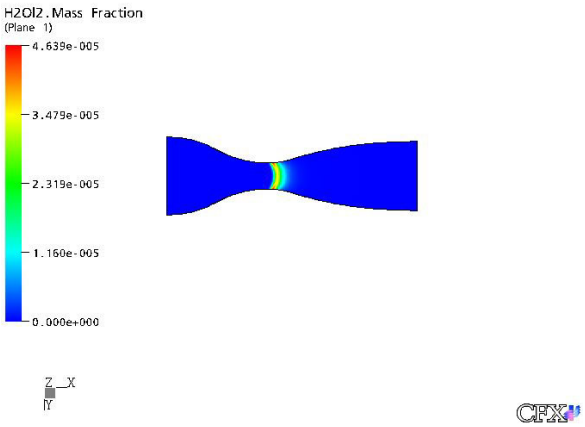

Figure 8b: Liquid Mass Fraction, Band 2, G1 Nozzle

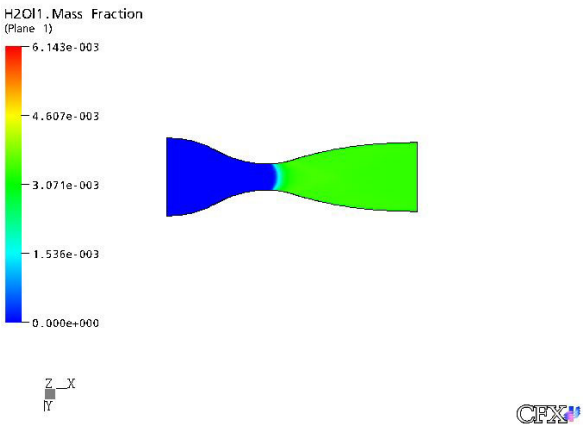

Figure 9a: Liquid Mass Fraction, Band 1, No Break-Up model

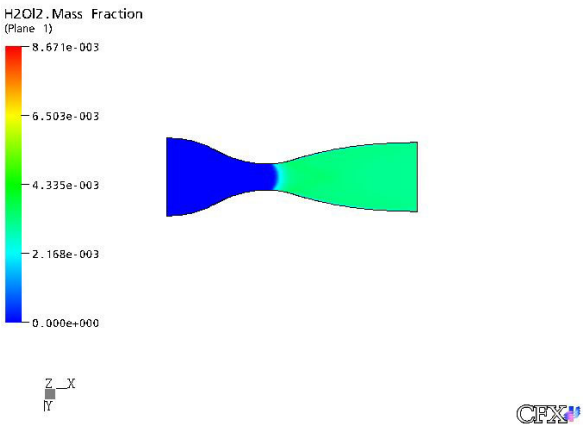

Figure 9b: Liquid Mass Fraction, Band 2, No Break-Up model